International Journal of Applied Science and Engineering
2014. 12, 4: 313-321

Fabrication and Characteristics of 8YSZ/Ni Functionally Graded Materials by Applying Spark Plasma Sintering Procedure

Mahmoud Samir EL-Wazery* and Ahmed Reffat EI-Desouky

Department of Production Engineering and Mechanical Design, Faculty of Engineering, Menoufiya University, Shebin El-Kom, Egypt

Abstract: Functionally graded materials (FGM) in the form of layered structure consisting of yttria stabilized zirconia (YSZ) and nickel were fabricated by spark plasma sintering procedure. The relative density, linear shrinkage and Vickers hardness of each layer of graded materials were measured. The microstructure and the composition of these components were studied. The results obtained show that functionally graded materials produced by spark plasma sintering exhibited a low porosity level and consequently fully dense specimens. Also, the results demonstrate that the composition and microstructure of YSZ/Ni FGM have the expected gradient distribution. There are no macroscopic distinct interfaces in YSZ/Ni FGM due to the gradient change in components. This good continuity of microstructure can eliminate the disadvantage of traditional macroscopic interface in YSZ/Ni joint, and reflect the design idea of FGM. Vicker's hardness of YSZ/Ni is lower than that of pure zirconia (YSZ) and increases by increasing the relative density of the layer of YSZ/Ni.

Keywords: Functionally graded materials (FGM); yttria stabilized zirconia (YSZ); spark plasma sintering (SPS); relative density and Microstructure.

1. Introduction

The concept of functionally graded materials (FGM), first proposed in the mid-1980s in Japan [1], is based on the development of compositional and/or microstructural gradients within the material leading towards graded properties in one, two or three dimensions [2, 3]. Compared to monolithic and composite materials, these structures offer the possibility of improving performance of components under demanding technological applications, e.g. in fuse-large surfaces of spacecraft, thermal and environmental barrier coatings for turbines and engines, super-hard cutting tools or artificial bones [4]. The zirconia/nickel FGMs can be designed to reduce thermal stresses and take advantage of the heat and corrosion resistances of ceramic and the mechanical strength, high toughness, good machinability and bonding capability of metals without severe internal thermal stresses. YSZ/Ni FGM are an ideal solution to the problem of metal–ceramic bonding [5-7].

Spark plasma sintering (SPS) is a newly developed process which makes possible sintering

* Corresponding author; e-mail: melwazery@ymail.com

Received 17 January 2014
Revised 19 September 2014
Accepted 22 September 2014

high quality materials in short periods by charging the intervals between powder particles with electrical energy. SPS systems offer many advantages (ex. rapid sintering, sintering less additives, uniform sintering, low running cost, easily operation) over conventional systems using hot press sintering, hot isostatic pressing or atmospheric furnaces process applies to many advanced material, functionally graded materials, fine ceramics, amorphous materials, target materials, thermoelectric generator. Local sintering rates can also be equalized by sintering in a temperature gradient which can be produced by laser surface heating or plasma-activated sintering in a stepped or tapered dies.

8-mol% yttria-stabilized zirconia (8YSZ) is widely chosen as the electrolyte in solid oxide fuel cells (SOFCs) because of its excellent high temperature ionic conductivity and excellent mechanical properties [8-10]. The influence of YSZ content and sintering temperature on microstructures and mechanical properties of Al_2O_3/YSZ composites was investigated by Menga et al. [11]. All samples could be fully densified at a temperature lower than 1400 $^{\circ}$C. Vickers hardness and fracture toughness of composites increased with increasing YSZ content, and the samples containing 10 wt.% of YSZ had the highest Vickers hardness of 18GPa. The mechanical properties of Si_3N_4–Al_2O_3 FGM joints with 15 layers for high-temperature applications were investigated [12]. Scanning electron microscopy (SEM) observations of fracture surfaces indicated the absence of any glassy phase at the triple points. This result was quite contrary to the previously reported 20-layer Al_2O_3/Si_3N_4 FGM samples where three-point bend testing revealed severe strength degradation at high temperatures. Shahrjerdi et al. [13] have demonstrated the functionally graded metal-ceramic composite fabricated via pressureless sintering. The pure metallic and ceramic components were Titanium (Ti) and Hydroxyapatite (HA), which were located at the ends of a cylindrical specimen. The properties of all FGM products were characterized by shrinkage, optical microscope (OM), SEM, energy dispersive spectrometry (EDX) and hardness test. The grade of the FGM material was proven by results from all recorded measurements, as well as linearity of shrinkage. The microstructure and mechanical properties of PSZ/NiCr FGMs fabricated by powder metallurgy were investigated experimentally. It was found that hardness increases and ductility decreases with the increase of partially stabilized zirconia (PSZ), which is attributed to the variation of the matrix phase from the metal to the ceramic [14]. Zhou and Li [15] have introduced the inverse homogenization for FGM microstructure design, where layered periodic base cells (PBC) were topologically optimized individually for specific graded properties. To ensure connectivity between different PBCs, heat sinks were prescribed on the PBC boundaries for maximizing their conduction. Lia et al. [16] have fabricated YSZ–FGM–NiCr joints by hot pressing process and studied their thermal properties by thermal cycling test and shear testing. The joint showed good thermal stability and good oxidation resistance up to 1000˚C. Also, Mishina et al. [17] studied the fabrication method of another constituent, PSZ/AISI316L FGMs by applying SPS procedure for use in joint prostheses and their mechanical and biotribological properties were evaluated through fracture toughness, bending strength, and Vicker hardness studies.

In this article, FGMs consisting of yttria stabilized zirconia (YSZ) and Ni were fabricated by spark plasma sintering procedure. The relative density, linear shrinkage and Vickers hardness of the FGM were studied. The compositional and microstructure analysis of all samples sets was examined after the sintering process through X-ray diffraction (XRD) and scanning electron microscopic (SEM) with energy dispersive X-ray analysis (EDAX). Vickers hardness was measured by performing indentations at a load of 5 kg within a dwell time of 15 s on the synthesized samples.

2. Expermental procedure

2.1. Materials

Yttria stabilized zirconia (8 mol. % Y_2O_3) powder (TOSOH, Japan) and Ni powder (MERK, USA) were used as the raw powders to fabricate the FGMs by utilizing the powder metallurgy technique. The mean particle sizes of powders were 0.5 μm for the YSZ and 15 μm for Ni, respectively. The YSZ and Ni powders were mixed in weigh ratios of 10:0, 9:1, 8:2, 7:3, 6:4 and 5:5, respectively. The composition of each layer in graded material is shown in Figure 1, and each mixture was suspended in alcohol, milled for five hrs by horizontal ball miller. The ratio of powder to ball was 1:2 and the milling speed was 100 r.p.m. 30 wt.% ethyl alcohol was added to the mixtures powders to cover the media (balls). After milling, the mixed powders were sieved using a 125 μm steel mesh to remove the remaining agglomerates. 10wt. % ethyl alcohol, as a lubricant, was added to the powders to form pure ceramic and intermediated layers. Then, the mixture powders were dried in a furnace at 70 ºC for 24 hrs. The powder blends were put to form a non-graded composition or were layered so as to form graded composition in a rectangular hot work tool steel die with 35 mm length and 10 mm width. The powder compacts were pressed up to 0.5 MPa at room temperature for one minute. Hydraulic press was used to compact the powder layers once at the same pressure. The die and punch set-up used to produce the non-graded composites (NGC) and FGM are reviewed in our paper [18-19]. Using the same pressing conditions, a larger thickness (6.5 mm) FGM green compact was also formed but under lower pressure (0.1MPa) during stacking the layers, which would be used for mechanical property testing.

100 wt. % YSZ	**Layer 1**
90 wt. % YSZ+ 10 wt. % Ni	**Layer 2**
80 wt. % YSZ+ 20 wt. % Ni	**Layer 3**
70 wt. % YSZ+ 30 wt. % Ni	**Layer 4**
60 wt. % YSZ+ 40 wt. % Ni	**Layer 5**
50 wt. % YSZ+ 50 wt. % Ni	**Layer 6**

Figure 1. composition distribution model of YSZ/Ni FGM

In the SPS process a green compact of the FGM was placed inside the plasma electrode, Figure 2. It applies large DC pulsed current (3 kA) directly to the green compact of FGM layers. Large DC pulsed current is considered to generate sparks between the powder particles and eventual repeat of momentary ultra-high temperature (1400 °C) under vacuum for one hour. The high frequency transfers and disperses the heat phenomena throughout the FGM specimen, resulting in a rapid and thorough heat distribution, high homogeneity and especially strong bonds between particles.

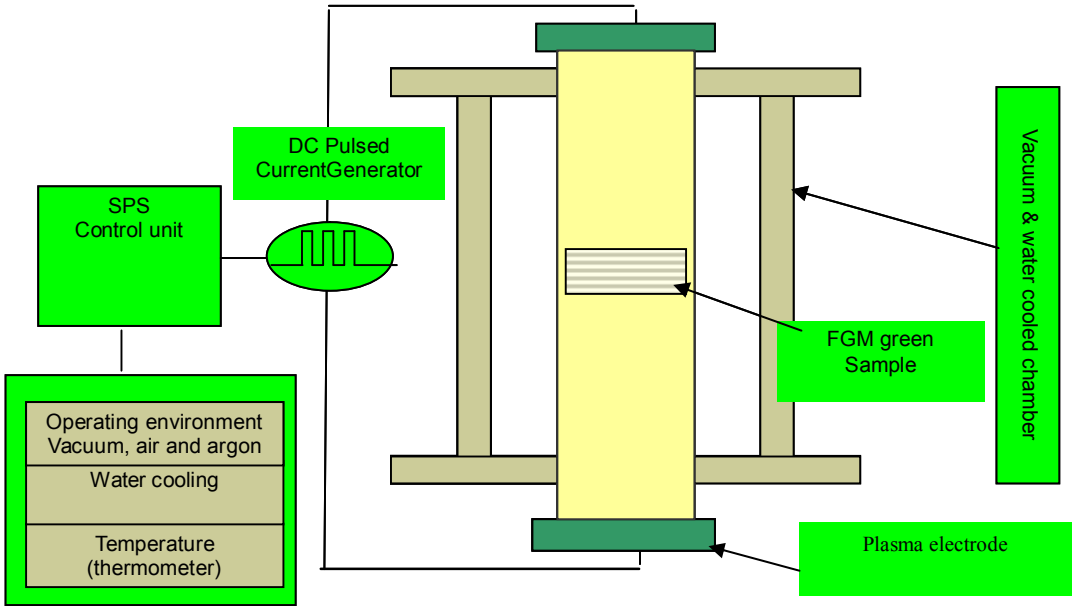

Figure 2. SPS system configuration

2.2. Materials Characterization

The actual density and the theoretical density of the sintered specimens were measured by using the water immersion method (Archimedes method) and the rule of mixture, respectively. The radial shrinkage of the NGC was measured by the thermo-mechanical analyzer (TMA-50 Shimadzu-Japan). The composition and microstructures of each layer of the graded materials specimens were examined by X-ray diffraction (XRD) and the scanning electron microscope (SEM-JSM 5400) with energy dispersive X-ray analysis (EDAX). A hardness tester (HSV-40) was used to measure the Vickers hardness of each layer in the YSZ/Ni FGM.

3. Results and discussion

3.1. Microstructure and XRD

Figure 3(a) shows the microstructure of the fabricated YSZ/Ni FGM. It has six layers: a pure YSZ layer and five YSZ/Ni composite layers containing 10, 20, 30, 40 and 50% of Ni, Figure 3(b). The white and gray regions exhibit the Ni and YSZ phases, respectively. The white area in each composite shows the nickel phase in a grayish YSZ matrix. The white area increased with increasing Ni contents from 0 to 50 wt.% and no distinct boundaries are exhibited. It can be seen that metal particles are homogeneously distributed into the ceramic matrix and there is no evidence of agglomerates. As the particle size of the zirconia powder was considerably smaller than that of the Ni powders, zirconia particles would have entered gaps between Ni particles on the fabrication. As a result, the Ni particles are dispersed in the zirconia matrix in the material with high content of Ni (40%Ni and 50%Ni).

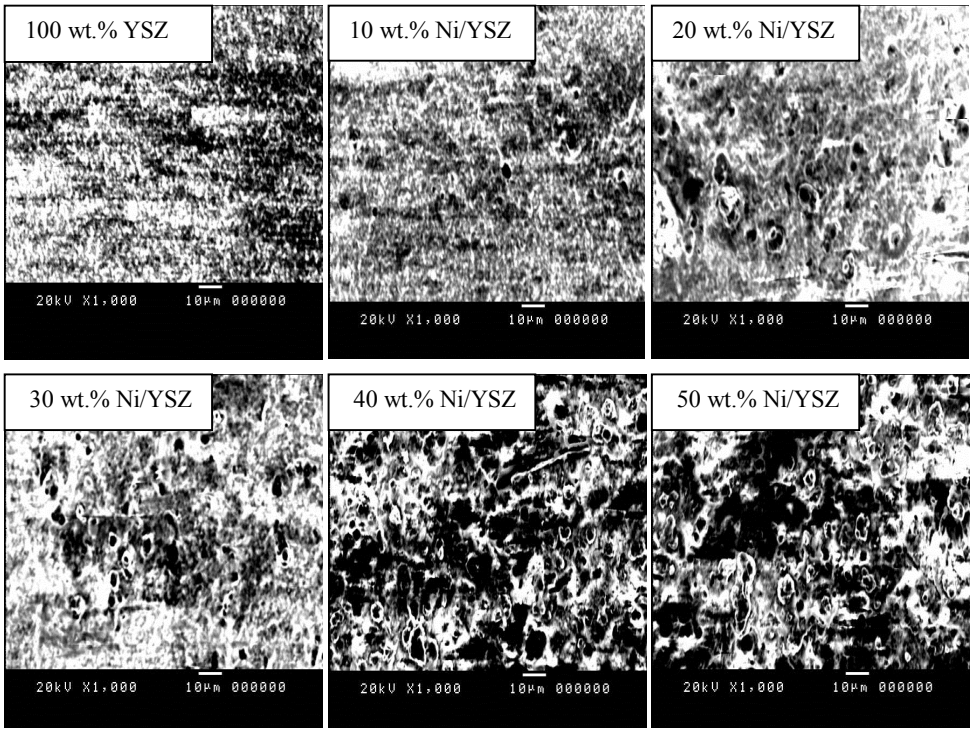

Figure 3(a). The micrographs of the FGM layers (gray part is nickel in YSZ)

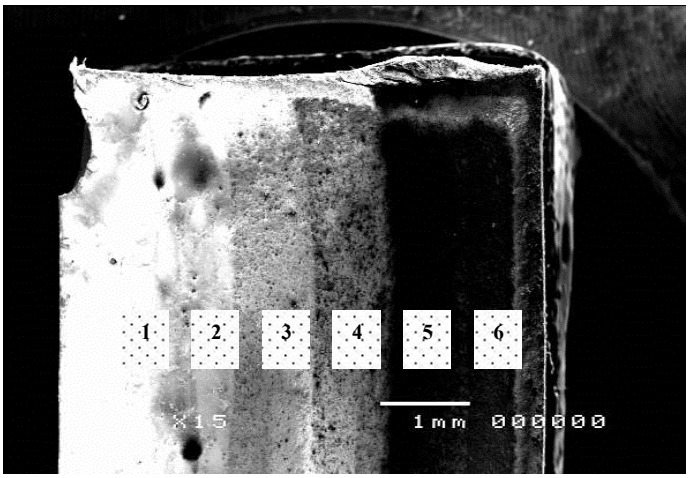

Figure 3(b). SEM images of the layers of the YSZ/Ni FGM

The X-ray diffraction patterns (XRD) from the surface of the cross-section for the NGCs (YSZ/40% Ni) after the spark plasma sintering under vacuum at 1400 ºC for one hour are shown in Figure 4. No new phase was formed between zirconia and Ni during sintering process. No other impurities above the detection limit have been detected.

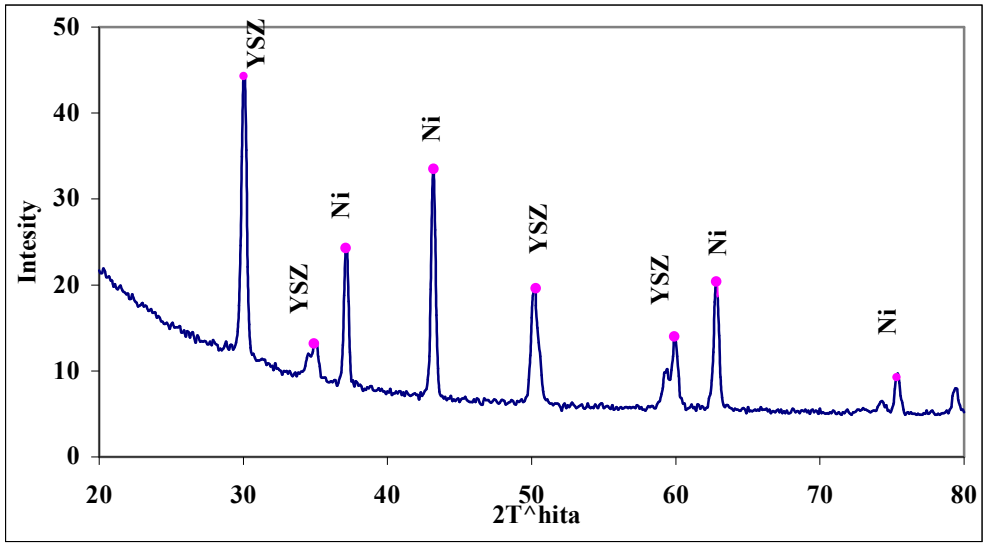

Figure 4. XRD patterns from the surface of the cross-section of the NGCs (YSZ/40%Ni)

3.2. Densification behavior

In the powder metallurgy process, the pores can be treated as the initiate defects. The relative densities of the layers in homogenous specimens and the YSZ/Ni FGM compacts are shown in Figure 5. Spark plasma sintering is an effective method to produce full dense specimens. It is noted that relatively high density (in the range of 0.90–0.99) for each layer in the FGM was obtained after the spark plasma sintering stage. The relative density has a maximum value (99%) for the pure YSZ and a minimum value (89.87%) for the homogeneous specimen with 50% nickel. Among the layers, layer 1 has the highest relative density, which is mainly attributed to a small initial particle size (0.5 μm) of zirconia selected for making the ceramic layer (pure ceramic layer) of the model structures. The higher relative density of zirconia is mainly due to its higher melting point, higher sinterability and hence higher sintering temperature for attaining fast densification than nickel. Among the five composite layers, the relative density decreases with increasing the content of nickel and the level of porosity is increased. Such effect can be attributed to the decrease in sintrability of Ni as well as its large particle size (15 μm). The FGMs exhibit a low porosity level and a relatively high relative density 99% by SPS procedure. The high value of the relative density of the YSZ/Ni FGM is related to the high densification, high homogeneity, rapid temperature increase and good bonding between the layers of FGM.

An important factor, which should be considered when analyzing the sinterability of YSZ/Ni FGM is the accurate prediction of the change in thermo-mechanical properties as shrinkage at each temperature. The thermal expansions coefficient of the Ni and the YSZ were (α_{Ni} =15.4 x10^{-6} °C^{-1} and α_{YSZ} = 7 x10^{-6} °C^{-1}), respectively [20]. The TMA was carried out on the layers of the FGM in air with a heating rate of 5˚C/min up to 1400 ˚C. To indirectly estimate the linear shrinkage of the layers in the FGMs fabricated by a spark plasma sintering procedure, the shrinkages of the NGC corresponding to each layer were measured by the thermo mechanical analyzer (TMA-50, Shimadzu-Japan) and the results were shown in Figure 6. It could be seen that the maximal value of linear shrinkage among the layers specimens is 19% for 10%Ni/YSZ. Among the other NGC layers, the linear shrinkage decreases with increasing the content of nickel and reached the minimum linear shrinkage (7%) at 50% Ni. This is because the lower sinterability of nickel compared to YSZ.

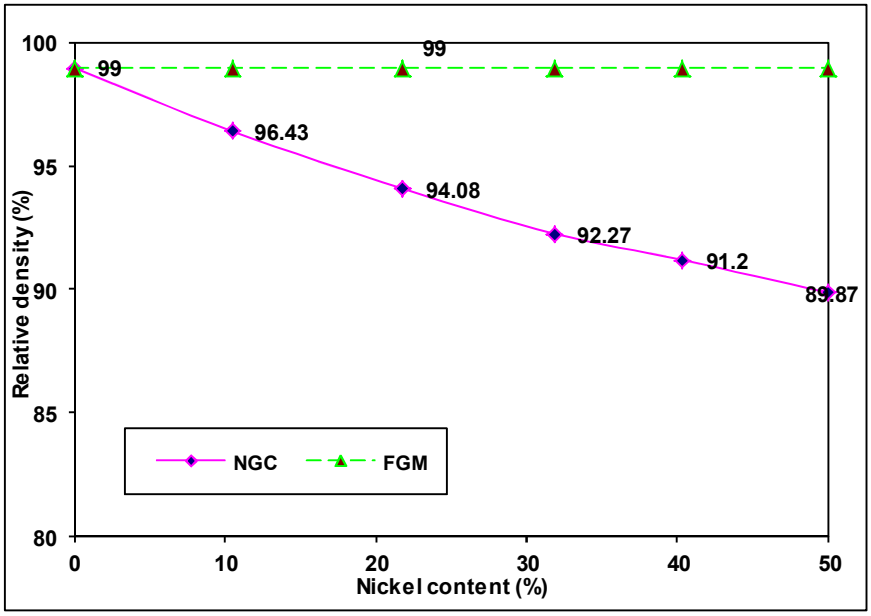

Figure 5. The relative densities of the non-graded composite and FGM specimens

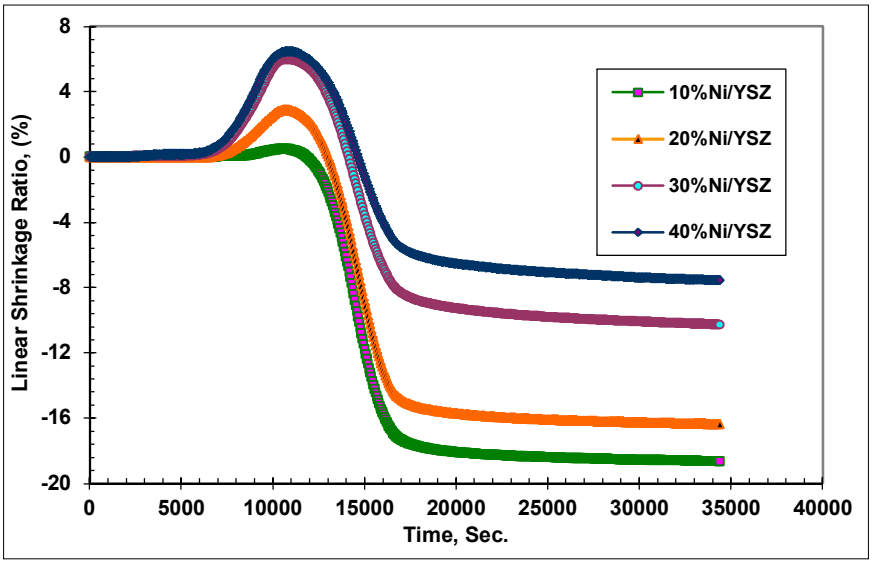

Figure 6. Relation between linear shrinkage and time of the FGM layers

3.3. Mechanical properties

The Vickers hardness of the YSZ/Ni FGM was measured using a hardness tester (HSV-40) on a polished surface under a load of 5 kg at 30 sec. The average of five indentations in each layer at the center and was used to calculate the hardness values of the layers. The Vickers hardness has a maximum value (15GPa) for the pure YSZ and a minimum value (5GPa) for the homogeneous specimen with 50% nickel (Figure 7).

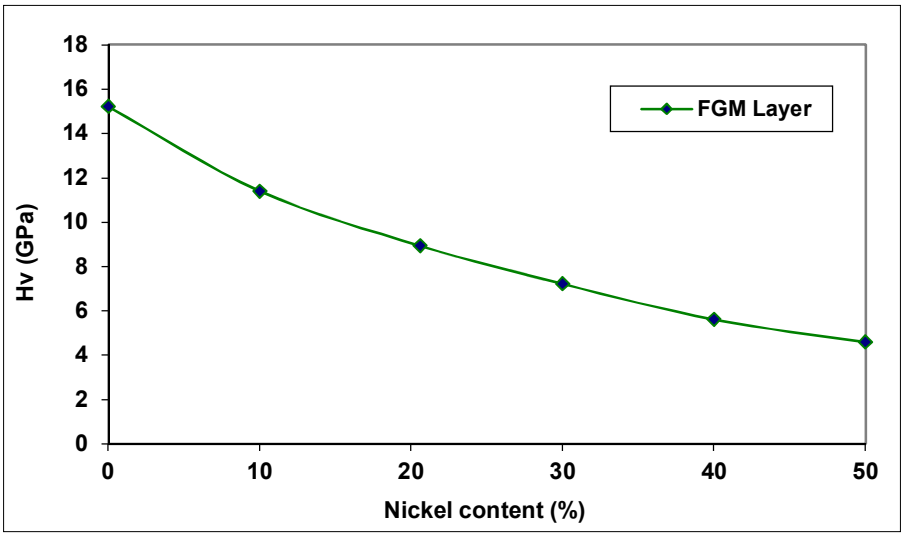

Figure 7. Vickers hardness of the layers in YSZ/Ni FGM

Also, it should be noted that the vickers hardness decreased with increasing nickel content. This is mainly attributed to the pores in intermediate layers in the FGM after sintering stage, where the pores were increased in the FGM layers with increasing nickel content from 0% to 50% Ni and the relative density was decreased also. Furthermore, hardness was reduced as the transformation from pure ceramic layer (YSZ) to intermediate layers (mixtures of zirconia and nickel powders) took place.

4. Conclusions

The spark plasma sintering (SPS) seems to be an effective method to obtain the full dense specimens. The FGMs exhibit a low porosity level and high relative density (99%). There are no macroscopic distinct interfaces in YSZ/Ni FGM due to the gradient change in components. This good continuity of microstructure can eliminate the disadvantage of traditional macroscopic interface in YSZ/Ni joint, and reflect the design idea of FGM. The linear shrinkage of the NGC was reduced with an increase in nickel content. There are more dimples in the microstructure resulted from agglomeration of nickel (metal) leaved from place in 50% NGC. Vicker's hardness of YSZ/Ni is lower than that of pure zirconia (YSZ) and increases by increasing the relative density of the layer of YSZ/Ni.

References

[1] Yamanouchi, M., Hirai, T., and Shiota, I. 1990. *Proceedings of the First International Symposium on Functionally Gradient Materials.* FGM Forum, Tokyo, Japan.

[2] Neubrand, A. and Rodel, J. 1997. Gradient materials: an overview of a novel concept, *Z Metallkd*, 88 , 358–371.

[3] Kieback, B., Neubrand, A., and Riedel, H. 2003. Processing technique for functionally graded material. *Material Science Engineering and Structure*, 362: 81-105.

[4] Miyamoto, Y., Kaysser, A., Rabin, B., and Kawasaki, A. 1999. "Functionally graded materials: *design processing and applications"*. Kluwer, Dordrecht, the Netherlands, Ford RG.

[5] Wosko, M. and Prazmowska, J. 2006. AIII-BV(N) Photodetectors with functionally graded active area. *Proceedings of the Symposium on Photonics Technologies for 7th Framework Program Wroclaw*, 12-14.
[6] Kawasaki, A. and Watanabe, R. 2002. Thermal fracture behavior of metal/ceramic functionally graded materials. *Engineering Fracture Mechanics*, 69: 1713–1728.
[7] Ruys, J., Popov, B., Sun, D., Russell, J., and Murray, J. 2001. Functionally graded electrical/thermal ceramic systems. *Journal of the European Ceramic Society*, 21: 2025–2029.
[8] Matula, G., Jardiel, T., Jimene, R., Levenfeld, B., and Várez, A. 2008. Microstructure, mechanical and electrical properties of Ni-YSZ anode supported solid oxide fuel cells. *International Journal of Materials Science and Engineering*, 32: 21-25.
[9] Rajeswari, K., Buchi, M., Hareesh, U., Srinivasa, Y., Das, R., and Johnson, R. 2011. Studies on ionic conductivity of stabilized zirconia ceramics (8YSZ) densified through conventional and non-conventional sintering methodologies. *Ceramics Internationa*, l37: 3557–3564.
[10] Yu, J., Park, W., Lee, S., and Woo, K. 2008. Microstructural effects on the electrical and mechanical properties of Ni-YSZ cermets for SOFC anode. *Power Sources*, 163: 921- 926.
[11] Menga, F., Liua, C., Zhangb, F., Tiana, Z., and Huanga, W. 2012. Densification and mechanical properties of fine-grained Al_2O_3–ZrO_2 composites consolidated by spark plasma sintering. *Journal of Alloys and Compounds*, 512: 63–67.
[12] Lee, S., Lemberg, A., Cho, G., Roh, Y., and Ritchie, O. 2010. Mechanical properties of Si_3N_4–Al_2O_3 FGM joints with 15 layers for high-temperature applications. *Journal of the European Ceramic Society*, 30: 1743–1749.
[13] Shahrjerdi, A., Mustapha, F., Bayat, M., Sapuan, S., and Majid, A. 2011. Fabrication of functionally graded hydroxyapatite-titanium by applying optimal sintering procedure and powder metallurgy. *International Journal of the Physical Sciences*, 6: 2258-2267
[14] Wu, Li., Jin, X., Sun, Y., and Guo, L. 2009. Microstructure and mechanical properties of ZrO_2/NiCr functionally graded materials. *Materials Science and Engineering A*, 509: 63–68.
[15] Zhou, S. and Li, Q. 2008. Microstructural design of connective base cells for functionally graded materials. *Materials Letters*, 62: 4022–4024
[16] Lia, J., Zenga, X., Tanga, N., and Xiaob, P. 2003 Fabrication and thermal properties of a YSZ–NiCr joint with an interlayer of YSZ–NiCr functionally graded material. *Journal of European Ceramic Society*, 23: 1847–1853.
[17] Mishina, H., Inumaru, Y., and Kaitoku, K. 2008. Fabrication of ZrO_2/AISI316L functionally graded materials for joint prostheses. *Materials Science and Engineering A*, 475: 141–147.
[18] EL-Wazery, S. M., EL-Desouky, R. A., Hamed, A. O., Mansour, A. N., and Hassan, A. A. 2012. Fabrication and mechanical properties of zirconia/nickel functionally graded materials. *International Journal of Advanced Materials Research*, 463-464, 463-47.
[19] EL-Desouky, A. R. and EL-Wazery, M. S., 2013. Mixed Mode Crack Propagation of Zirconia/ Nickel Functionally Graded Materials. *International Journal of Engineering (IJE)*, 26: 885-894.
[20] Jingchuan, Z., Zhongda, Y., Zhonghong, L., and Jian, L. 1996. Microstructure and thermal relaxation of ZrO_2/Ni functionally graded materials. *Trans. Nonferrous Met. Soc. China,* 6: 94-99.